A Mechanistic and Kinetic Study of the E-Ring Hydrolysis and Lactonization of a Novel Phosphoryloxymethyl Prodrug of Camptothecin

Bradley A. Hanson,[1,2] Richard L. Schowen,[1] and Valentino J. Stella[1,3]

Received January 2, 2003; accepted March 31, 2003

Purpose. This study was done to determine the E-ring hydrolysis and lactonization mechanism of a water-soluble 20-phosphoryloxymethyl (POM) prodrug of camptothecin (P-CPT). Specifically, the role of the phosphate group in facilitating E-ring hydrolysis was examined.

Methods. Resolution between the lactone and carboxylate forms of P-CPT and camptothecin (CPT) was achieved with a RPHPLC assay using UV-visible detection. E-ring P-CPT hydrolysis and lactonization kinetics were followed using 20 mM acetate or phosphate buffer (μ = 0.15 NaCl) over the pH range of 4 to 8 at 25.0°C. A kinetic solvent isotope effect (KSIE) study was used to further probe the mechanism of E-ring hydrolysis.

Results. The hydrolysis and lactonization reactions followed pseudo-first-order kinetics in the approach to equilibrium. The equilibrium ratio of the open and closed forms of P-CPT was dependent on pH, with the closed form dominant at low pH and the open form dominant at high pH. Buffer concentration changes had little to no effect on the rate of P-CPT E-ring hydrolysis. The KSIE study provided an overall isotope effect of 2.47 and a proton inventory KSIE consistent with an intramolecular general base catalysis.

Conclusions. P-CPT has a pH-dependent equilibrium between the lactone and carboxylate forms similar but not identical to that of CPT. The results suggest a hydrolysis reaction mechanism that involves a single site hydrogen exchange facilitated intramolecularly by the dianionic phosphate moiety of P-CPT via either general base catalysis of the lactone ring attack by water or breakdown of the tetrahedral intermediate.

KEY WORDS: camptothecin; phosphoryloxymethyl (POM) prodrug; hydrolysis; lactonization; kinetic solvent isotope effects; stability.

INTRODUCTION

An investigation of the mechanism of hydrolysis and lactonization of a novel, water-soluble 20-phosphoryloxymethyl (POM) prodrug of camptothecin (P-CPT, Scheme 1C) for comparison with available information on camptothecin (CPT, Scheme 1) (1) is reported. CPT is a naturally occurring cytotoxic alkaloid first isolated by Wall and Wani in 1966 from the Chinese plant *Camptotheca accuminata* (2). CPT and CPT derivatives have shown anticancer activity *in vitro* and *in vivo* (2–13). The anticancer activity of CPT results from its inhibition of the DNA topoisomerase I enzyme, which is essential for DNA relaxation during replication, transcription, and repair (14,15). Recent studies have suggested that CPT may bind noncovalently to the enzyme–DNA complex initially, and subsequent nucleophilic attack by the enzyme at the acyl position of the E-ring may stabilize the covalent ternary complex (11,16,17).

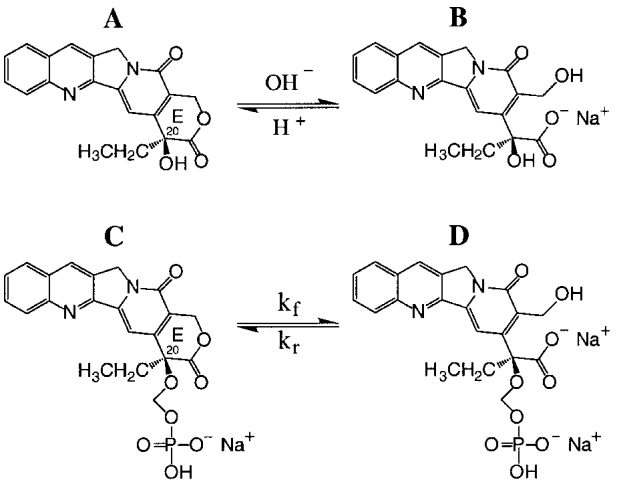

Scheme 1. The pH-dependent equilibrium between the lactone (A) and the carboxylate (B) forms of CPT. The pH-dependent equilibrium between the lactone (C) and the carboxylate (D) forms of P-CPT. The rate constants k_f and k_r are the forward (hydrolysis) and reverse (lactonization) rate constants for the lactone–carboxylate equilibrium, respectively.

The affinity of CPT for topoisomerase I led to renewed interest in this class of drugs in the early 1990s, after an earlier phase I clinical trial of the sodium carboxylate form of CPT (Scheme 1B) in the 1970s were discontinued because of apparent low activity and severe toxicity (18–20). CPT itself is sparingly soluble (2–3 μg/mL) (2). CPT with an intact lactone E-ring was later found to be 10 times more potent than the sodium carboxylate form (5,21,22). However, the pH-dependent equilibrium between the lactone and carboxylate forms shifts toward the less potent carboxylate form under physiologic conditions (2). Previously in our laboratory, the hydrolysis and lactonization mechanisms for CPT were studied in detail (1), confirming the pH-dependent equilibrium between lactone and carboxylate and documenting the rapid hydrolysis of CPT to the inactive carboxylate form.

In the phosphoryloxymethyl (POM) prodrug of CPT (P-CPT), the POM functional group is attached to the 20-OH group on the E-ring of CPT (Scheme 1C). The POM functional group has been successfully used for prodrug design in our laboratory previously and appeared ideal for CPT (23–26). The main problem that has plagued CPT is its low aqueous solubility and facile E-ring hydrolysis, which limited the ability to deliver the active lactone form *in vivo* (2). P-CPT was intended to circumvent these problems as well as to provide a safe means of CPT delivery via rapid cleavage of the POM group by alkaline phosphatases (23–26).

Previous work indicated that the 20-OH group contributes to increased biologic activity and chemical reactivity of the lactone (2,27,28). Unpublished results in our laboratory have shown that alkylation of the 20-OH by either a methyl or methyl thiomethyl ($-CH_2SCH_3$) group depressed the rate of

[1] Department of Pharmaceutical Chemistry, The University of Kansas, Lawrence, Kansas 66047.
[2] Ann Arbor Laboratories, Pfizer Inc., Ann Arbor, Michigan 48105.
[3] To whom correspondence should be addressed. (e-mail: stella@ku.edu)

0724-8741/03/0700-1031/0 © 2003 Plenum Publishing Corporation

E-ring opening. By analogy, it was hypothesized that blocking the 20-OH group with a POM moiety would also stabilize the lactone E-ring against hydrolysis. This could allow P-CPT(closed) to be formulated and to convert to CPT(closed) quantitatively *in vivo*, thus delivering the active form of CPT by the action of alkaline phosphatases. The influence of the POM group on E-ring hydrolysis is reported here because, as will be seen, the terminal phosphate group was found to be catalyze E-ring hydrolysis. The findings here point to pH values where P-CPT may be formulated in its lactone form but also provide basic insight into the role of intramolecular catalysis by phosphate groups. Future papers will address the physicochemical characterization (solubility, long-term stability at pH 4, pK_a determination, etc.) and pharmacokinetics of P-CPT.

MATERIALS AND METHODS

Chemicals

CPT was donated by Dabur India Ltd. (New Delhi, India). P-CPT was synthesized by Dr. Jan Zygmunt in the Center for Drug Delivery Research at The University of Kansas and used without further purification (29). Monobasic sodium phosphate, dibasic sodium phosphate, sodium acetate trihydrate, glacial acetic acid, sodium chloride, and acetonitrile (HPLC grade UV cutoff 190 nm) were all ACS certified and were purchased from Fisher Scientific (Pittsburgh, PA). Tetrabutylammonium dihyrdrogenphosphate (1.0 M in water), deuterium oxide (D_2O, 99.9% D), and deuterated dimethylsulfoxide (DMSO-d_6, 99.9% D) were purchased from Aldrich Chemical Company (Milwaukee, WI). Dimethyl sulfoxide (DMSO) was purchased from Tera Pharmaceuticals, Inc. (Buena Park, CA). All chemicals were used without further purification. All water was purified with a LABCONCO (Kansas City, MO) Water Pro PS system.

HPLC Analysis

Separation of the open and closed forms of P-CPT and CPT was accomplished by reversed-phase HPLC using a Shimadzu instrument consisting of a Shimadzu LC-6A solvent delivery module, a Shimadzu SPD-6A UV spectrophotometric detector, a Shimadzu SCL-6A system controller, a Shimadzu C-R6A Chromatopac integrator (Shimadzu Corp., Kyoto, Japan), and a Rheodyne loop injector (Rheodyne, Cotati, CA). An octadecyl silane (ODS) Hypersil® (150 mm × 4.6 mm id, 5 μm) HPLC column was used to separate the compounds. The analysis used a 20-μl injection loop, UV detection at 350 nm, and a flow rate of 2.0 ml/min. The mobile phase consisted of 25 mM pH 6.5 phosphate (NaH_2PO_4/Na_2HPO_4) buffer, acetonitrile, and 1.0 M tetrabutylammonium dihydrogenphosphate (750:250:16, v/v/v). A buffer pH of 6.5 was used to minimize on-column conversion of CPT (1) and P-CPT between the closed and open forms. The buffer pH (pD) and all other solutions were monitored using a Corning (Medfield, MA) pH/ion meter (Model 155) with a Corning General Purpose Combination pH electrode.

The HPLC assay was optimized by following the equilibration reactions of a P-CPT (2 μg/ml; 4.4 μM) and CPT (2 μg/ml; 5.7 μM) solution in 25 mM pH 8 sodium phosphate buffer (μ = 0.15 NaCl). CPT analysis was performed to see if any CPT was formed during the time that P-CPT ring opening and closing was being studied. No CPT was found to form. Sample solutions (2 μg/ml) of each compound were followed separately to equilibrium by HPLC in order to validate the identity of each peak on the chromatogram. Retention volumes were 7.6 ml [CPT(closed), Scheme 1, A], 8.8 ml [CPT (opened), B], 14.6 ml [P-CPT (closed), C], and 11.2 ml [P-CPT (opened), D]. The conditions given above (particularly pH and ion-pairing agent) led to full baseline resolution and elution of both forms of CPT and P-CPT within 8 min.

Calibration curves for both forms of P-CPT were linear over the closed concentration range of 0.3–11 × 10^{-6} M. P-CPT closed and open standards were diluted with 20 mM pH 4 acetate and 20 mM pH 8 phosphate buffer, respectively. The method for preparing the standards was analogous to the procedure to produce the kinetic solutions (see below).

P-CPT Interconversion Kinetics in H_2O and D_2O

The *in vitro* kinetic studies were performed in aqueous buffer solutions at 25 ± 0.1°C maintained by a Precision shaking water bath (Model 50). Hydrolysis (E-ring opening) and lactonization (E-ring closing) of P-CPT were studied in the pH range 4–8 at pH increments of 0.5. Acetate (20 mM, pH range 4–6) and phosphate buffers (20 mM, pH 6.5–8) were used to maintain pH. Kinetic studies in the pH range 6 to 8 using 10 and 40 mM acetate (pH 6) and phosphate (pH 6.5–8) buffers were performed to determine the effect, if any, buffer concentration would have on P-CPT hydrolysis. The ionic strength (μ) value of all solutions was adjusted to 0.15 M by the addition of NaCl. Studies were performed in triplicate unless otherwise noted.

P-CPT hydrolysis was initiated by addition of 50 μL of P-CPT stock solution (0.5 mg/ml) in DMSO to a 10-ml volumetric flask and dilution with acetate (pH 6) or phosphate (pH 6.5–8) buffer to produce an initial substrate concentration of 2.5 μg/ml (5.5 μM). P-CPT lactonization was initiated by addition of 100 μl of a P-CPT/NaOH solution (see below) to a 10-ml volumetric flask and dilution with acetate buffer (pH 4–5.5) to produce an initial substrate concentration of 2.5 μg/ml (5.5 μM). The P-CPT/NaOH solution consisted of equal volumes of P-CPT stock solution (0.5 mg/ml) in DMSO and 10 mM NaOH solution in water, which was allowed to stand for 30 min to produce the carboxylate form of P-CPT (no conversion of P-CPT to CPT was noted in preparing and on storage of this solution). The final DMSO concentration was 0.5% (v/v) in the reaction solutions. The pH of the sample solutions was determined before and after each kinetic experiment; the variation was less than 0.05 pH units.

Kinetic solvent isotope effects (KSIE) for P-CPT hydrolysis were obtained from observed rate constants (k_{obs}) measured in H_2O and D_2O. The KSIE is defined as k_{H2O}/k_{D2O}, where k_{H2O} and k_{D2O} are the k_{obs} values in H_2O and D_2O, respectively. P-CPT hydrolysis was initiated by adding 50 μl of a P-CPT stock solution (0.5 mg/ml) in DMSO-d_6 to a 10-ml volumetric flask and dilution with sodium phosphate buffer in D_2O (pD range of 6–7.5) to produce an initial substrate concentration of 2.5 μg/ml (5.5 μM). The pD was determined from Eq. 1 (30):

$$pD = (\text{meter reading}) + 0.4 \quad (1)$$

where "meter reading" refers to the value read from a glass-

electrode pH meter after temperature correction. At pH 7.5, hydrolysis studies were performed in 20 mM phosphate buffer using a 50:50 weight fraction H_2O:D_2O. The pL was calculated from Eq. 2 (30):

$$pL = 0.076n^2 + 0.3314n \quad (2)$$

where pL is the negative logarithm of the sum of all lyonium-ion concentrations and n is the atom fraction of deuterium (n = 0.5 for 50:50 H_2O:D_2O). The "meter reading" after temperature correction was equivalent to 7.5 minus pL (30). The ionic strength was adjusted to 0.15 M (NaCl), and duplicate trials were performed for each pH value.

Aliquots of the reaction solutions were withdrawn periodically, and both forms of P-CPT were determined by HPLC. The reactions were monitored by the appearance and disappearance of the open and closed forms, respectively. Below pH 6, the appearance and disappearance of the closed and open forms were followed, respectively. Values of k_{obs} were determined from the negative slope of plots of ln $|A_{eq} - A_t|$ vs. time (t), where A_{eq} is the peak area of either reactant or product at equilibrium (>10 half-lives) and A_t is the peak area at time t. The k_{obs} values from each experiment were averaged.

The equilibrium concentration of P-CPT(closed) {$[P\text{-}CPT(closed)]_{eq}$} was determined at each pH from A_{eq} using a calibration curve for P-CPT(closed). The P-CPT(opened) equilibrium concentration {$[P\text{-}CPT(opened)]_{eq}$} was calculated as the difference between the P-CPT(closed) initial and equilibrium concentrations. P-CPT lactone is considered the E-ring closed form, and the P-CPT carboxylate is the E-ring opened form that can be in its protonated (carboxylic acid) or unprotonated (carboxylate) state. Values of rate and equilibrium constants (see Scheme 2) k_r (lactonization or reverse rate constant), k_f (hydrolysis or forward rate constant), and K_{obs} (observed equilibrium constant) were calculated from Eqs. 3–6 (1,31):

$$k_{obs} = k_r + k_f \quad (3)$$

$$K_{obs} = \frac{k_f}{k_r} = \frac{[P - CPT(opened)]_{eq}}{[P - CPT(closed)]_{eq}} \quad (4)$$

$$k_r = \frac{k_{obs}}{K_{obs} + 1} \quad (5)$$

$$k_f = k_{obs} - k_r \quad (6)$$

All values are the average of three trials (two in deuterated solvents). The rate constants k_r and k_f for H_2O were fitted (SigmaPlot® 4.14) to Eqs. 7 and 8 given below. The parameter values with standard errors of the mean are shown in Scheme 2.

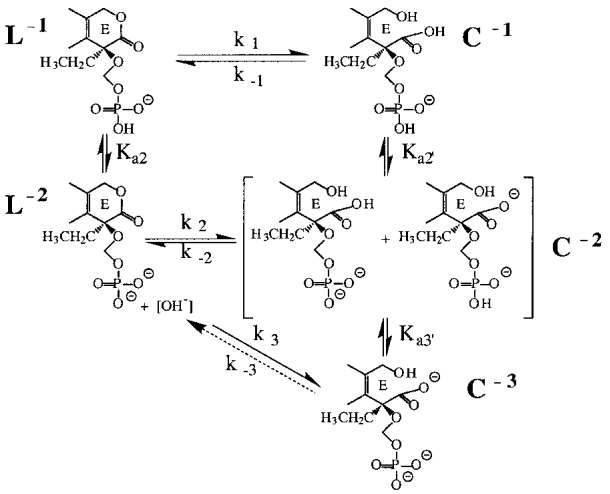

Hydrolysis	Lactonization
k_1 = 1.58 (± 0.53) x 10^{-4} min^{-1}	k_{-1} = 7.50 (± 0.43) x 10^{-2} min^{-1}
k_2 = 4.41 (± 0.09) x 10^{-3} min^{-1}	k_{-2} = 3.43 (± 0.19) x 10^{-3} min^{-1}
k_3 = 962 (± 131) M^{-1} min^{-1}	$K_{a2'}$ = 1.87 (± 0.18) x 10^{-4} M
K_{a2} = 9.79 (± 0.89) x 10^{-7} M	$pK_{a2'}$ = 3.73 (± 0.04)
pK_{a2} = 6.01 (± 0.04)	$K_{a3'}$ = 2.88 (± 0.51) x 10^{-7} M
	$pK_{a3'}$ = 6.54 (± 0.08)

Scheme 2. Proposed reaction scheme for the hydrolysis (k_f) and lactonization (k_r) of P-CPT. With use of SigmaPlot®, the lactonization and hydrolysis parameters were determined by fitting the data to Eqs. 7 and 8, respectively, corresponding to this reaction scheme. The parentheses contain the standard errors of the mean.

RESULTS AND DISCUSSION

pH Dependence of the Equilibrium between P-CPT(Closed) and P-CPT(Opened)

P-CPT hydrolysis was studied in H_2O and D_2O at 25°C with the ionic strength held constant at 0.15 M with NaCl. The k_{obs} values for the hydrolysis of P-CPT(closed) in H_2O and D_2O solutions at various pH (pD) values and buffer concentrations are listed in Table I. Buffer catalysis of P-CPT hydrolysis was examined in a limited pH range. The variations in k_{obs} with buffer concentration were small and do not support significant buffer catalysis. In further work, a constant buffer concentration of 20 mM was used.

The equilibrium constants K_{obs} for interconversion of the open and closed forms of P-CPT (Eq. 4) are displayed in Table II. The K_{obs} values for P-CPT E-ring opening increase as pH increased in the pH range of 4–8. Plotting the percent of $[P\text{-}CPT(closed)]_{eq}$ and $[P\text{-}CPT(opened)]_{eq}$ vs. pH (Fig. 1A) shows the pH dependence of the equilibrium of P-CPT. As pH increases, the dominant species shifts from P-CPT(closed) to P-CPT(opened) with the percentage of each species being equivalent at pH 6.15 where K_{obs} = 1 (Fig. 1A). Scheme 1 shows that hydroxide drives the E-ring opening of CPT (1,2) and presumably accounts for the pH dependence seen in Fig. 1A. However, the pH dependence cannot be fit by a simple ionization equation as the sigmoidal curve of the data in Fig. 1A might suggest. The situation is best approached through the kinetics analysis described below for k_r and k_f. In addition, the majority of the P-CPT(opened) form is in its carboxylate form above pH 6.15, rather than the carboxylic acid, because of the estimated pK_a of 3.73 ± 0.04 for $pK_{a2'}$ (Scheme 2).

The k_{obs} and K_{obs} values, along with Eqs. 5 and 6, were used to calculate k_r and k_f. Plotting k_r and k_f vs. pH (Fig. 1B) shows the pH dependence of the P-CPT lactonization and hydrolysis reactions. As pH increases, the largest contribution to k_{obs} shifts from k_r to k_f, with the two rate constants being equivalent when K_{obs} = 1 at pH 6.15. The best-fit lines in Fig. 1B were derived by fitting k_r and k_f to Eqs. 7 and 8, respectively, using SigmaPlot® (discussed in more detail in the next section). The k_r and k_f values derived by fitting were used to

Table I. Values of k_{obs} and KSIE for Equilibration between the Open and Closed Forms of P-CPT in H_2O and D_2O at 25°C

Solvent	pH	Buffer	[M]	*n*	k_{obs} (min^{-1})	KSIE[a]
H_2O	4.0	Acetate	0.02	3	$2.83\ (\pm0.07) \times 10^{-2}$[d,f]	
	4.5	Acetate	0.02	3	$1.40\ (\pm0.02) \times 10^{-2}$[d,f]	
	5.0	Acetate	0.02	3	$7.61\ (\pm0.11) \times 10^{-3}$[d,f]	
	5.5	Acetate	0.02	3	$5.36\ (\pm0.03) \times 10^{-3}$[d,f]	
	6.0	Acetate	0.01	3	$4.65\ (\pm0.26) \times 10^{-3}$[e,f]	
			0.02	3	$5.32\ (\pm0.02) \times 10^{-3}$[e,f]	
			0.04	3	$5.20\ (\pm0.05) \times 10^{-3}$[e,f]	
	6.5	Phosphate	0.02	3	$5.18\ (\pm0.06) \times 10^{-3}$[e,f]	
	7.0	Phosphate	0.01	3	$4.94\ (\pm0.07) \times 10^{-3}$[e,f]	
			0.02	3	$4.91\ (\pm0.15) \times 10^{-3}$[e,f]	
			0.04	3	$5.08\ (\pm0.08) \times 10^{-3}$[e,f]	
	7.5	Phosphate	0.01	2	$4.90\ (\pm0.01) \times 10^{-3}$[e,g]	
			0.02	3	$4.98\ (\pm0.14) \times 10^{-3}$[e,f]	
			0.04	2	$5.07\ (\pm0.01) \times 10^{-3}$[e,g]	
	8.0	Phosphate	0.01	3	$5.38\ (\pm0.11) \times 10^{-3}$[e,f]	
			0.02	3	$5.43\ (\pm0.03) \times 10^{-3}$[e,f]	
			0.04	3	$5.53\ (\pm0.04) \times 10^{-3}$[e,f]	
D_2O	6.0[b]	Phosphate	0.02	2	$2.60\ (\pm0.04) \times 10^{-3}$[e,g]	2.05
	6.5[b]	Phosphate	0.02	2	$1.98\ (\pm0.03) \times 10^{-3}$[e,g]	2.62
	7.0[b]	Phosphate	0.02	2	$1.99\ (\pm0.01) \times 10^{-3}$[e,g]	2.47
	7.5[b]	Phosphate	0.02	2	$2.02\ (\pm0.01) \times 10^{-3}$[e,g]	2.47
	7.5[b,c]	Phosphate	0.02	2	$3.40\ (\pm0.01) \times 10^{-3}$[e,g]	

Note: The errors are displayed as range or standard deviation (SD) for experiments performed in duplicate or triplicate, respectively.
[a] KSIE value as described in the text.
[b] pD.
[c] 50:50 weight fraction of H_2O:D_2O.
[d] The average value (and range or SD) determined from monitoring the disappearance of the carboxylate and the appearance of the lactone.
[e] The average value (and range or SD) determined from monitoring the appearance of the carboxylate and the disappearance of the lactone.
[f] Errors calculated as SD.
[g] Errors displayed as range.

address the pH dependence of P-CPT equilibrium seen in Fig. 1A. The solid lines in Fig. 1A represent the ratio of k_r and k_f (Eq. 4) in percent for $[\text{P-CPT(closed)}]_{eq}$ and the ratio of k_f and k_r (inverse of Eq. 4) in percent for $[\text{P-CPT(opened)}]_{eq}$. These results are similar to CPT (1) because a pH-dependent lactone–carboxylate equilibrium is evident, and the open forms of both compounds are dominant above pH 8. However, CPT differs from P-CPT in that the $K_{obs} = 1$ at approximately pH 7 (6.15 for P-CPT), and the closed form of CPT is dominant below pH 4.5 (5 for P-CPT) (1).

pH Dependence of the Interconversion Kinetics of P-CPT(Closed) and P-CPT(Opened)

The lactone ring cleavage mechanism of CPT proposed by Fassberg *et al.* (1) provided insight into the acyl cleavage of the lactone ring and the lack of substituent effects on the A-ring. The addition of a POM promoiety on the E-ring at the 20-OH position of CPT changes the mechanism considerably. A reaction scheme for the hydrolysis and lactonization of P-CPT (Scheme 2) is proposed. The rate expressions based on the reaction scheme shown in Scheme 2 for the lactonization (k_r) and hydrolysis (k_f) rate constants are defined by Eqs. 7 and 8, respectively.

$$k_r = k_{-1}\, f_{C^{-1}} + k_{-2}\, f_{C^{-2}} = \frac{k_{-1}\,[H^+]^2 + k_{-2}\,[H^+]\,K_{a2'}}{[H^+]^2 + [H^+]\,K_{a2'} + K_{a2'}\,K_{a3'}} \quad (7)$$

$$k_f = k_1\, f_{L^{-1}} + k_2\, f_{L^{-2}} + k_3\,[OH^-]\, f_{L^{-2}} = \frac{k_1\,[H^+] + k_2\,K_{a2} + k_3\,[OH^-]\,K_{a2}}{[H^+]\,K_{a2}} \quad (8)$$

In Eq. 7, k_{-1} and k_{-2} are the rate constants for the lactonization of the monoanionic (C^{-1}) and dianionic (C^{-2}) P-CPT(opened) forms, respectively. The fractions of monoanionic and dianionic P-CPT(opened) present at a given pH value are represented, respectively, by $f_{C\text{-}1}$ and $f_{C\text{-}2}$. $K_{a2'}$ and $K_{a3'}$ are the acid dissociation constants for the monoanionic and two indistinguishable dianionic P-CPT(opened) species and the two indistinguishable dianionic and trianionic (C^{-3}) P-CPT(opened) forms, respectively. In Eq. 8, k_1, k_2, and k_3 are the rate constant for the hydrolysis of the monoanionic (L^{-1}) P-CPT(closed) form, the rate constant for the hydrolysis of the dianionic (L^{-2}) P-CPT(closed) form, and the hydroxide ion-catalyzed rate constant for the hydrolysis of the dianionic P-CPT(closed) form, respectively. The fractions of monoanionic and dianionic P-CPT(closed) present at a given pH value are represented, respectively, by $f_{L\text{-}1}$ and $f_{L\text{-}2}$. K_{a2} is the acid dissociation constant for the monoanionic and dianionic P-CPT(closed) forms. The parameter values and the standard error of the mean are located in Scheme 2 under the Hydrolysis and Lactonization headings.

Plots of k_r, k_f and the best-fit lines based on SigmaPlot®-derived values from Eqs. 7 and 8 vs. pH are displayed in Fig. 1B. The rate expressions appear to provide an adequate interpretation of the P-CPT hydrolysis and lactonization reactions. The hydrolysis reaction parameters (Scheme 2 under Hydrolysis) are reasonable if each parameter is rationalized according to the reaction scheme and rate expressions. The k_2 value is an order of magnitude larger than the k_1 value, which would agree with the observation that as pH increases, the k_f value receives a larger contribution from the dianionic P-

Table II. Equilibrium Percentages of P-CPT (Closed) and P-CPT (Opened) and Values of K_{obs} for Equilibration between P-CPT Forms in H_2O and D_2O at 25°C

Solvent	pH	P-CPT (% Closed ± error)	P-CPT Open (% Open ± error)	K_{obs}[a]
H_2O	4.0[b]	100.0 ± 0.0[f]	0.0 ± 0.0[f]	—[f,h]
	4.5[b]	97.9 ± 0.4[f]	2.1 ± 0.4[f]	0.0215 ± 0.0047[f]
	5.0[b]	90.6 ± 1.1[f]	9.4 ± 1.1[f]	0.104 ± 0.013[f]
	5.5[b]	76.1 ± 0.5[f]	23.9 ± 0.5[f]	0.315 ± 0.009[f]
	6.0[b]	59.3 ± 1.8[f]	40.7 ± 1.8[f]	0.688 ± 0.051[f]
	6.5[c]	35.7 ± 0.4[f]	64.3 ± 0.4[f]	1.80 ± 0.03[f]
	7.0[c]	16.1 ± 0.8[f]	83.9 ± 0.8[f]	5.23 ± 0.33[f]
	7.5[c]	6.9 ± 0.7[f]	93.1 ± 0.7[f]	13.5 ± 1.6[f]
	8.0[c]	2.3 ± 0.1[f]	97.7 ± 0.1[f]	43.0 ± 2.0[f]
D_2O	6.0[c,d]	84.1 ± 0.2[g]	15.9 ± 0.2[g]	0.189 ± 0.003[g]
	6.5[c,d]	62.2 ± 0.9[g]	37.8 ± 0.9[g]	0.608 ± 0.024[g]
	7.0[c,d]	37.3 ± 0.3[g]	62.7 ± 0.3[g]	1.68 ± 0.02[g]
	7.5[c,d]	18.2 ± 0.3[g]	81.8 ± 0.3[g]	4.49 ± 0.08[g]
	7.5[c,d,e]	10.4 ± 0.2[g]	89.6 ± 0.2[g]	8.65 ± 0.20[g]

Note: The errors are displayed as SD for H_2O experiments performed in triplicate and as range for D_2O experiments performed in duplicate.
[a] K_{obs} as described in the text.
[b] 20 mM acetate buffer.
[c] 20 mM phosphate buffer.
[d] pD.
[e] 50:50 weight fraction of H_2O: D_2O.
[f] Errors calculated as SD.
[g] Errors displayed as range.
[h] The observed equilibrium constant appears to be zero. However, based on the ratio k_f/k_r and using the k_f [1.99 (± 0.05) × 10^{-4}] value from the k_f curve fit (Fig. 2), the K_{obs} at pH 4 is estimated to be 0.00703, i.e., about 0.7% of P-CPT exists in an open form at pH 4.

CPT(closed) form (Fig. 1B). The pK_{a2} value of 6.01 ± 0.04 is consistent with literature values for the second pK_a of monoalkyl phosphates (32) and, more specifically, a value of 6.31 for the second pK_a of methyl phosphate (33). The lactonization reaction parameters (Scheme 2 under Lactonization) define the reverse of the hydrolysis reaction. The k_{-1} value is an order of magnitude larger than the k_{-2} value, which agrees with the observation that as pH decreases, the k_r value receives a larger contribution from the monoanionic P-CPT(opened) form (Fig. 1B). The $pK_{a2'}$ value of 3.73 ± 0.04 is reasonable because the reaction scheme depicts the acid dissociation of a carboxylic acid with a typical pK_a of 3.5–4.0. This is also consistent with pK_a values of 3.65 for α-hydroxybutyric acid (34) and 3.77 for D-gluconic acid (35). The $pK_{a3'}$ value of 6.54 ± 0.08 is consistent for the second acid dissociation constant of the phosphate group. On estimation of the two pK_a values from the curve fitting, the two indistinguishable dianionic P-CPT(opened) forms can be replaced by the dianionic P-CPT(opened) form with a carboxylate and monoanionic phosphate group (right structure within the brackets of C^{-2}). However, on lactonization of the dianionic P-CPT(opened) form, the other structure containing the dianionic phosphate and carboxylic acid would be consistent with the ring closing to the dianionic P-CPT(closed) form. The lactonization of the trianionic P-CPT(opened) form to the dianionic P-CPT(closed) form was not included in Eq. 7 because the contribution to lactonization appears to be negligible at pH values well above 6.5. The reaction scheme, rate expressions, and excellent fit of the data provide a consistent mechanistic profile of P-CPT hydrolysis and lactonization.

Catalysis of the Interconversion of P-CPT and KSIE

The plot of k_{obs} values for P-CPT and CPT hydrolysis to equilibrium (1) as a function of pH is displayed in Fig. 2. The solid line in Fig. 2 represents the addition of the P-CPT k_r and k_f values (Eq. 3) where k_r and k_f were derived by fitting the k_r and k_f values to Eqs. 7 and 8 (Fig. 1B), respectively. P-CPT hydrolysis is actually enhanced compared to CPT (pH range of 4–7). The k_{obs} values from CPT and P-CPT hydrolysis were compared using 20 mM buffer concentrations at 25°C because the P-CPT values were not extrapolated to zero buffer concentration. CPT k_{obs} values at 20 mM buffer concentrations were obtained by extrapolating to this concentration using the data from the CPT study (1).

Some of the original goals in creating P-CPT were to slow down the E-ring hydrolysis by alkylating the 20-OH group, to increase the water solubility, and to provide a larger amount of the active lactone form of CPT after cleavage of the POM promoiety. Obviously, the first goal of greater E-ring stability was not attained (see Fig. 2). A reason for the enhanced E-ring reactivity in P-CPT might be the participation of the phosphate group in catalyzing the hydrolysis. This would be consistent with the pH-rate profile and the relative magnitudes of rate constants displayed in Fig. 2. If the phosphate group was participating in catalyzing the E-ring hydrolysis, insight into this mechanism could be gleaned by performing a KSIE study.

A primary solvent isotope effect of about 2.5 was observed in the pH range 6–7.5 for P-CPT hydrolysis (Table I). If the phosphate group were catalyzing the reaction by a nucleophilic attack (Scheme 3A) on the E-ring ester function to form a mixed anhydride, the expected KSIE should be 1.0; i.e., no proton would be transferred in the rate-determining step. This would be inconsistent with the observed KSIE value of 2.47. Therefore, catalysis by nucleophilic attack of the phosphate group at the lactone carbonyl center can be reasonably ruled out.

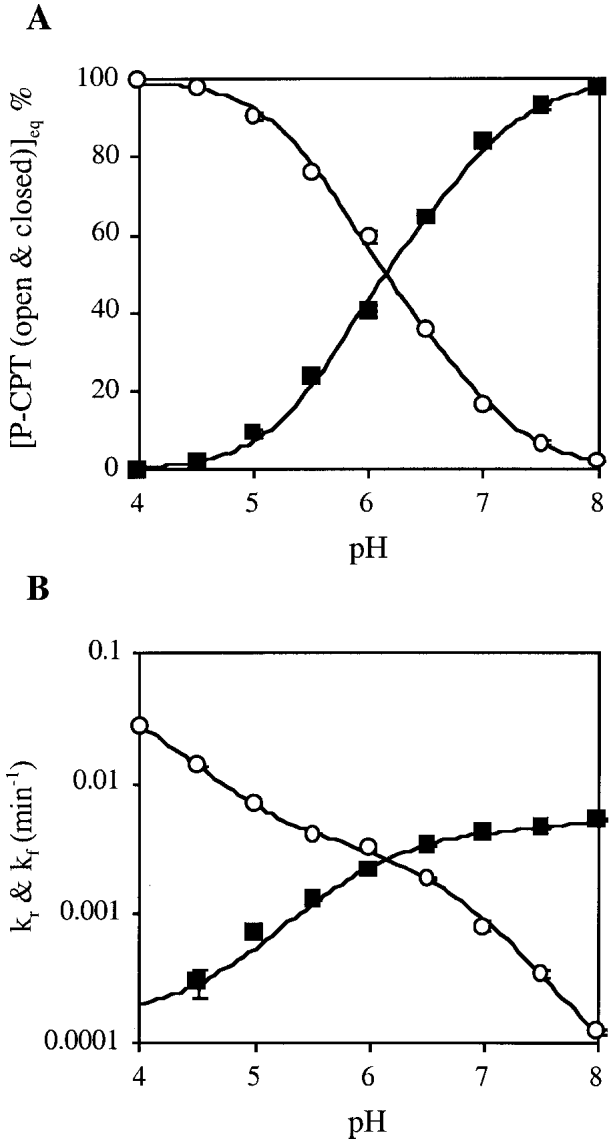

Fig. 1. Plots showing (A) the percent of P-CPT(closed) (○) and P-CPT(opened) (■) at equilibrium vs. pH and (B) the pH-rate profiles for k_r (○) and k_f (■) for the lactonization and hydrolysis of P-CPT (25°C; 20 mM buffer; μ = 0.15M NaCl). In B, the k_r and k_f values were obtained by fit using SigmaPlot® to Eqs. 7 and 8, respectively, corresponding to the proposed reaction scheme (see Scheme 2). The solid lines represent the best fit of the data to the equations. The solid lines in A represent the ratio of k_r and k_f (Eq. 4) in percent for $[\text{P-CPT(closed)}]_{eq}$ and the ratio of k_f and k_r (inverse of Eq. 4) in percent for $[\text{P-CPT(opened)}]_{eq}$. The k_r and k_f values were derived by fitting the k_r and k_f values to Eqs. 7 and 8 (Fig. 1B), respectively. The error bars represent standard deviations (SD). If error bars are not visible, the SD is less than the symbol size.

For further evaluation of the KSIE, a minimal proton inventory was constructed by measurement of k_{obs} at pH (pD) 7.5 for atom fractions of D in H_2O:D_2O mixtures, *n,* of 0, 0.5, and 1.0 (Fig. 3). The value of k_{obs} is independent of pH from pH 6 to pH 8. The simplest models (30) for these results would be:

$$k_n = k_0(1 - n + n\phi) \quad (9)$$

$$k_n = k_0(1 - n + n\phi^{0.5})^2 \quad (10)$$

$$k_n = k_0(1 - n + n\phi')Z^n \quad (11)$$

The k_n value is the k_{obs} where the *n* atom fraction of D in the H_2O:D_2O mixtures varies for H_2O (n = 0, k_0), 50:50 H_2O:D_2O solution (n = 0.5, $k_{0.5}$) and D_2O (n = 1, k_1). The ϕ value is defined by the ratio of k_1 and k_0. The ϕ' value is defined by the same ratio except that there are Z number of exchange sites as compared to one and two in Eqs. 9 and 10, respectively. Equation 9 corresponds to a simple general base catalysis with a single transition-state proton transfer site, Eq. 10 to general base catalysis through an intervening water molecule (two sites), and Eq. 11 to a single transition-state site combined with generalized solvation. All three models fit the data within experimental error, but the most general (Eq. 11) suggests an intramolecular general base catalytic site (k_H/k_D = 2.1) with a small solvation effect (k_H/k_D = 1.2). The phosphate group thus seems to be an intramolecular general base catalyst (Scheme 3B or 3C). No further effort was made to distinguish between tetrahedral breakdown (Scheme 3B) or formation (Scheme 3C) as the rate-determining step. Also not ruled out is the kinetically equivalent mechanism of intramolecular general acid catalysis by the phosphate group on hydroxide attack or breakdown of the monoanionic tetrahedral intermediate. However, these mechanisms intuitively seem less likely.

CONCLUSIONS

P-CPT has a pH-dependent equilibrium between the lactone and carboxylate forms that is similar to CPT. P-CPT lactone and carboxylate forms dominate the lactone–carboxylate equilibrium below pH 4.5 and above pH 8, respectively. The hydrolysis and lactonization reaction mechanisms for P-CPT were defined well by a reaction scheme and the corresponding rate expressions. The POM promoiety was found to have a considerable catalytic effect on the opening of

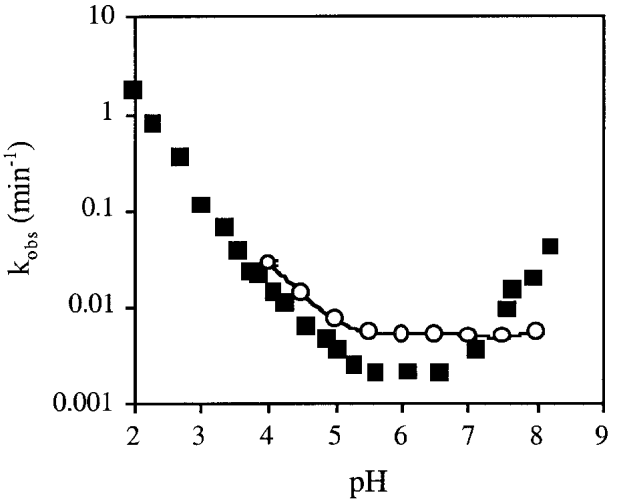

Fig. 2. The pH-rate profiles for the E-ring hydrolysis of CPT (■, 20 mM buffer; μ = 0.5 M NaCl) by Fassberg *et al.* (1) and P-CPT (○, 20 mM buffer; μ = 0.15 M NaCl) at 25°C. The solid line represents the addition of the P-CPT k_r and k_f values (Eq. 3), where k_r and k_f were derived by fitting the k_r and k_f values to Eqs. 7 and 8 (Fig. 1B), respectively. The error bars represent SD. If error bars are not visible, the SD is less than the symbol size.

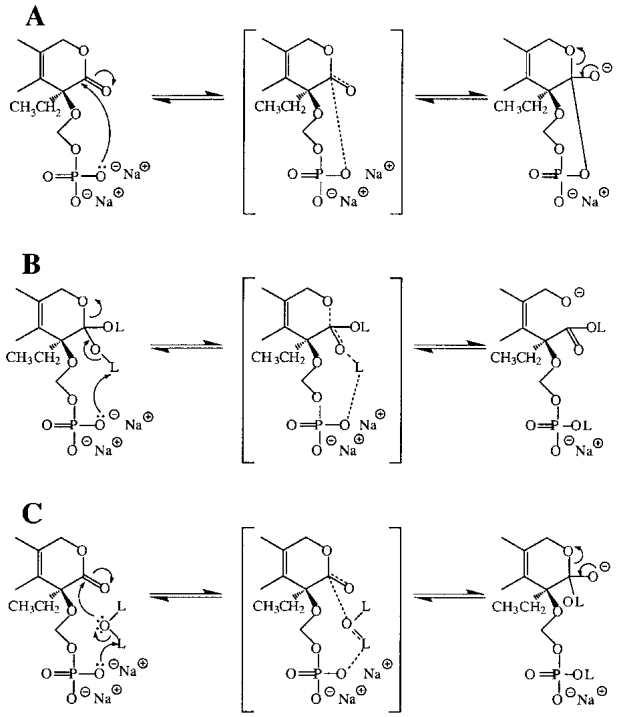

Scheme 3. Possible transition states of P-CPT hydrolysis including one (A) that lacks proton exchange (KSIE = 1) in producing a tetrahedral intermediate and two that involve a single proton exchange (KSIE = 2–3) via either (B) breakdown of the tetrahedral intermediate or (C) general base catalysis of the lactone ring attack by water.

the E-ring. An overall KSIE of 2.47 and a linear proton inventory study were evidence of a hydrolysis reaction involving a single site hydrogen facilitated by the dianionic phosphate moiety of P-CPT via either general base catalysis of the attack by water on the lactone ring or breakdown of the tetrahedral intermediate. Based on the fact that the P-CPT(lactone) form dominates below pH 4.5, future studies concentrated on formulating P-CPT for *in vivo* delivery at pH 4, where the solubility is >2.5 mg/ml.

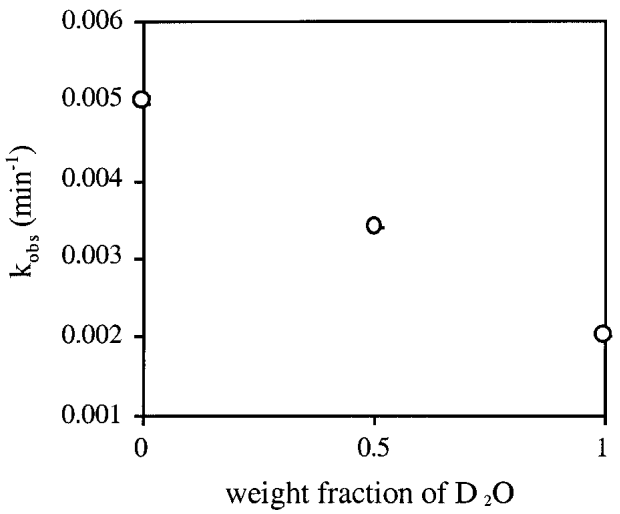

Fig. 3. k_{obs} (○) vs. weight fraction of D_2O (proton inventory plot) for P-CPT E-ring hydrolysis at 25°C (pL = 7.5; 20 mM phosphate buffer; μ = 0.15 M NaCl). The overall KSIE value is 2.47 under these experimental conditions. The error bars represent range. If error bars are not visible, the range is less than the symbol size.

ACKNOWLEDGMENTS

The authors gratefully acknowledge the financial support of the Schering Plough Predoctoral Fellowship, the Siegfried Lindenbaum Predoctoral Fellowship, the Center for Drug Delivery Research, the Kansas Technology Enterprise Corporation (KTEC), and The University of Kansas. The authors gratefully acknowledge Dr. Jan Zygmunt and Dr. Gunda Georg of the Department of Medicinal Chemistry at The University of Kansas for the synthesis of P-CPT and for offering CPT for this study.

REFERENCES

1. J. Fassberg and V. J. Stella. A kinetic and mechanistic study of the hydrolysis of camptothecin and some analogues. *J. Pharm. Sci.* **81**:676–684 (1992).
2. M. E. Wall, M. C. Wani, C. E. Cook, K. H. Palmer, A. T. McPhail, and G. A. Sim. Plant antitumor agents. I. The isolation and structure of camptothecin, a novel alkaloidal leukemia and tumor inhibitor from *Camptotheca acuminata. J. Am. Chem. Soc.* **88**:3888–3890 (1966).
3. M. C. Wani and M. E. Wall. Plant antitumor agents. II. The structure of two new alkaloids from *Camptotheca acuminata. J. Org. Chem.* **34**:1364–1367 (1969).
4. J. A. Adamovics and C. R. Hutchinson. Prodrug analogues of the antitumor alkaloid camptothecin. *J. Med. Chem.* **22**:310–314 (1979).
5. M. C. Wani, P. E. Ronman, J. T. Lindley, and M. E. Wall. Plant antitumor agents. 18. Synthesis and biological activity of camptothecin analogues. *J. Med. Chem.* **23**:554–560 (1980).
6. M. C. Wani, A. W. Nicholas, and M. E. Wall. Plant antitumor agents. 23. Synthesis and antileukemic activity of camptothecin analogues. *J. Med. Chem.* **29**:2358–2363 (1986).
7. M. C. Wani, A. W. Nicholas, G. Manikumar, and M. E. Wall. Plant antitumor agents. 25. Total synthesis and antileukemic activity of ring A substituted camptothecin analogues. Structure–activity correlations. *J. Med. Chem.* **30**:1774–1779 (1987).
8. W. Eng, L. Faucette, R. K. Johnson, and R. Sternglanz. Evidence that DNA topoisomerase I is necessary for the cytotoxic effects of camptothecin. *Mol. Pharmacol.* **34**:755–760 (1988).
9. C. Jaxel, K. W. Kohn, M. C. Wani, M. E. Wall, and Y. Pommier. Structure–activity study of the actions of camptothecin derivatives on mammalian topoisomerase I: Evidence for a specific receptor site and a relation to antitumor activity. *Cancer Res.* **49**: 1465–1469 (1989).
10. Y. Hsiang, L. F. Liu, M. E. Wall, M. C. Wani, A. W. Nicholas, G. Manikumar, S. Kirschenbaum, R. Silber, and M. Potmesil. DNA topoisomerase I-mediated DNA cleavage and cytotoxicity of camptothecin analogues. *Cancer Res.* **49**:4385–4389 (1989).
11. R. P. Hertzberg, M. J. Caranfa, and S. M. Hecht. On the mechanism of topoisomerase I inhibition by camptothecin: Evidence for binding to an enzyme–DNA complex. *Biochemistry* **28**:4629–4638 (1989).
12. Y. Hsiang, M. G. Lihou, and L. F. Liu. Arrest of replication forks by drug-stabilized topoisomerase I-DNA cleavable complexes as a mechanism of cell killing by camptothecin. *Cancer Res.* **49**: 5077–5082 (1989).
13. M. Bjornsti, P. Benedetti, G. A. Viglianti, and J. C. Wang. Expression of human DNA topoisomerase I in yeast cells lacking yeast DNA topoisomerase I: Restoration of sensitivity of the cells to the antitumor drug camptothecin. *Cancer Res.* **49**:6318–6323 (1989).
14. M. Gupta, A. Fujimori, and Y. Pommier. Eurkaryotic DNA topoisomerase I. *Biochim. Biophys. Acta* **1262**:1–14 (1995).
15. J. C. Wang. DNA topoisomerases. *Annu. Rev. Biochem.* **65**:635–692 (1996).
16. C. Jaxel, G. Capranico, D. Kerrigan, K. W. Kohn, and Y. Pommier. Effect of local DNA sequence on topoisomerase I cleavage

in the presence or absence of camptothecin. *J. Biol. Chem.* **266**: 20418–20423 (1991).
17. Y. Pommier, G. Kohlhagen, K. W. Kohn, F. Leteurtre, M. C. Wani, and M. E. Wall. Interaction of an alkylating camptothecin derivative with a DNA base at topoisomerase I-DNA cleavage sites. *Proc. Natl. Acad. Sci. USA* **92**:8861–8865 (1995).
18. J. A. Gottlieb and J. K. Luce. Treatment of malignant melanoma with camptothecin (NSC-100880). *Cancer Chemother. Rep.* **56**: 103–105 (1972).
19. F. M. Muggia, P. J. Creaven, H. H. Hansen, M. H. Cohen, and O. S. Selawry. Phase 1 clinical trial of weekly and daily treatment with camptothecin (NSC-100880): Correlation with preclinical studies. *Cancer Chemother. Rep.* **56**:515–521 (1972).
20. P. J. Creaven, L. M. Allen, and F. M. Muggia. Plasma camptothecin (NSC-100880) levels during a 5-day course of treatment: Relation to dose and toxicity. *Cancer Chemother. Rep.* **56**:573–578 (1972).
21. M. E. Wall and M. C. Wani. Antineoplastic agents from plants. *Annu. Rev. Pharmacol. Toxicol.* **17**:117–132 (1977).
22. R. P. Hertzberg, M. J. Caranfa, K. G. Holden, D. R. Jakas, G. Gallagher, M. R. Mattern, S. M. Mong, J. O. Bartus, R. K. Johnson, and W. D. Kingsbury. Modification of hydroxy lactone ring of camptothecin; inhibition of topoisomerase I and biological activity. *J. Med. Chem.* **32**:715–720 (1989).
23. M. Safadi, R. Olizai, and V. J. Stella. Phosphoryloxymethyl carbamates and carbonates—Novel water-soluble prodrugs for amines and hindered alcohols. *Pharm. Res.* **10**:1350–1355 (1993).
24. J. P. Krise, J. Zygmunt, G. I. Georg, and V. J. Stella. Novel prodrug approach for tertiary amines: Synthesis and preliminary evaluation of N-phosphonooxymethyl prodrugs. *J. Med. Chem.* **42**:3094–3100 (1999).
25. J. P. Krise, S. Narisawa, and V. J. Stella. A novel prodrug approach for tertiary amines. 2. Physiochemical and *in vitro* enzymatic evaluation of selected N-phosphonooxymethyl prodrugs. *J. Pharm. Sci.* **88**:922–927 (1999).
26. J. P. Krise, S. Narisawa, and V. J. Stella. A novel prodrug approach for tertiary amines. 3. *In vivo* evaluation of two N-phosphonooxymethyl prodrugs in rats and dogs. *J. Pharm. Sci.* **88**:928–932 (1999).
27. M. E. Wall. Plant antitumor agents. 5. Alkaloids with antitumor activity. In K. Mothes, K. Schrieber and H. R. Schulte (eds.), *International Symposium on Biochemistry and Physiology of the Alkaloids*, Academie-Verlag, Berlin, 1969, pp. 77–87.
28. A. W. Nicholas, M. C. Wani, G. Manikumar, M. E. Wall, K. W. Kohn, and Y. Pommier. Plant antitumor agents. 29. Synthesis and biological activity of ring D and ring E modified analogues of camptothecin. *J. Med. Chem.* **33**:972–978 (1990).
29. V. J. Stella, J. J. Zygmunt, I. G. Georg and M. S. Safadi. Water soluble prodrugs of hindered alcohols. United States Patent 6,204,257, March 20, 2001.
30. K. B. Schowen and R. L. Schowen. Solvent isotope effects on enzyme systems. *Methods Enzymol.* **87C**:551–606 (1982).
31. M. J. Kaufman. Rate and equilibrium constants for acid-catalyzed lactone hydrolysis of HMG-CoA reductase inhibitors. *Int. J. Pharm.* **66**:97–106 (1990).
32. J. Emsley and D. Hall. Reaction mechanisms. In J. Emsley (ed.), *The Chemistry of Phosphorus: Environmental, Organic, Inorganic, Biochemical, and Spectroscopic Aspects*, John Wiley & Sons, New York, 1976, pp. 232.
33. W. D. Kumler and J. J. Eiler. The acid strength of mono and diesters of phosphoric acid: The *n*-alkyl esters from methyl to butyl, the esters of biological importance and the natural guanidine phosphoric acids. *J. Am. Chem. Soc.* **65**:2355 (1943).
34. W. P. Jencks. and J. Regenstein. Physical and Chemical Data. In G. D. Fasman (ed.), *Handbook of Biochemistry and Molecular Biology*, CRC Press, Cleveland, 1976, pp. 310–342.
35. Y. Pocker and E. Green. Hydrolysis of D-glucono-δ-lactone. I. General acid-base catalysis, solvent deuterium isotope effects, and transition state characterization. *J. Am. Chem. Soc.* **95**:113–119 (1973).